

PHASE RELATIONSHIPS IN THE AL-RICH REGION OF THE Al-Y-Zr SYSTEM

X. Bao^{ab}, L. Liu^a, S. Huang^a, Y. Jiang^c, X. Wang^a, L. Zhang^{a*}^a School of Material Science and Engineering, Central South University, Changsha, Hunan, China^b State Key Laboratory of Powder Metallurgy, Central South University, Changsha, China^c College of Automotive and Mechanical Engineering, Changsha University of Science and Technology, Changsha, China

(Received 11 October 2015; accepted 22 June 2016)

Abstract

The phase relations in the Al-Y-Zr ternary system at 873 K have been investigated by X-ray powder diffraction (XRD) and scanning electron microscopy (SEM) with energy dispersive X-ray spectroscopy (EDS) in backscattered electron imaging (BSE) modes. Six three-phase equilibria are determined and no ternary compound is observed. In the meantime, first principle calculations are used to provide theoretical guidance to understand the experimental results.

Keywords: Phase diagram; Al-Y-Zr system; X-ray diffraction; Electron microscopy

1. Introduction

Due to the potential applications in automotive and aerospace industries, aluminum alloys have been extensively studied for decades. It has been reported that the addition of rare earth elements into aluminum alloys is an additional way to improve the properties of conventional aluminum alloys such as tensile strength, heat resistance and corrosion resistance, etc.[1-5]. Research shows that the addition of RE or Zr to the aluminum alloys can improve the high temperature properties of the alloys due to the formation of Al₃RE (L1₂-type (AuCu₃) structure) precipitates in the aluminum alloys which are able to be coherent or semi-coherent with the Al matrix [6-8]. The formation of stable or metastable L1₂-type (AuCu₃) Al₃RE phases could be the key to enhance the strength of Al-RE alloys [1,9,10]. Moreover, the addition of Y into aluminum alloys has been found to improve the mechanical property and glass forming ability of the alloy [11,12]. These preliminary findings lead to our experiments on the Al-Y-Zr ternary system.

Three relevant binary systems have been assessed and collected from Refs.[13-15] in Table 1, together with the available crystallographic data and stability temperature ranges of all the intermediate phases. At 873 K, there are eight binary compounds in the Al-Zr system, five in the Al-Y system and no compound in the Y-Zr system.

Recently, the phase equilibrium of the Al-Y-Zr ternary system at 773 K has been investigated by She

et al. [16]. No ternary compound was reported in this system.

Table 1. Crystal structure information of phases in Al-Y-Zr ternary system

Phase	Space Group	Lattice parameters		
		a	b	c
AlZr ₃	Pmm	0.43917(1)	-	-
AlZr ₂	P6 ₃ /mm	0.4894	-	0.5928
Al ₂ Zr ₃	P4 ₂ /mnm	0.7630(1)	-	0.69281(1)
Al ₃ Zr ₄	P	0.5433(2)	-	0.5390(2)
AlZr	Cmcm	0.3353	1.0866	0.4266
Al ₃ Zr ₂	Fdd2	0.9601(0)	1.3906(2)	0.5574
Al ₂ Zr	P6 ₃ /mmc	0.43601(2)	-	0.87482(5)
Al ₃ Zr	I4/mmm	0.4005	-	1.7285
Al ₃ Y _H	Rm	0.61884	-	2.1094
Al ₃ Y _L	P6 ₃ /mmc	0.6276	-	0.4582
Al ₂ Y	Fdm	0.78611	-	-
AlY	Cmcm	0.3884	1.1522	0.4385
Al ₂ Y ₃	P4 ₂ /mnm	0.82411	-	0.76411
AlY ₂	Pnma	0.654	0.508	0.94

* Corresponding author: ligangzhang@csu.edu.cn



2. Methods

In this work, the alloy buttons were prepared in an electric arc furnace under a pure argon atmosphere with a water-cooled cooper crucible. Six samples with various alloy compositions were selected to investigate the isothermal section of the Al-rich region in the Al-Y-Zr ternary system, and their compositions are listed in Table 2. The starting materials were used in the form of pieces of high purity elements: Al (99.99 wt. %), Zr (99.9 wt. %) and Y (99.9 wt. %). Titanium was used as an oxygen getter during the melting process. The ingots were re-melted five times to ensure their homogeneity. The weight loss was generally less than 1.0 % after melting (some alloys showed no weight loss at all). All the melted alloy samples were put into Silica capsules and annealed at 873 K for 1800 hours, hereafter the capsules were broken in ice water.

Scanning electron microscopy (SEM) with energy dispersive spectrometer (EDS) was used to analyze the microstructures of equilibrated alloys. Besides, powder X-ray diffraction (XRD) was applied to identify the crystal structure of key phases. The phase relationships in the Al-Y-Zr ternary system at 873 K were determined by a combination of these characterization techniques.

The enthalpies of formation of some compounds in this system were calculated by using first-principle calculations, which is run by utilizing the scalar relativistic all-electron Blöchl's projector augmented-wave (PAW) means [17,18] with the generalized gradient approximation (GGA). The Perdew-Bucke-Ernzerhof parameterization (PBE) [19,20] was adopted for the GGA exchange-correlation function. This calculation was achieved in the highly-efficient Vienna ab initio simulation package (VASP) [21,22].

3. Results and discussion

3.1 Phase analysis

The experimental investigation of the isothermal section at 873 K in this system mainly focuses on the Al-rich region. By analyzing and comparing the X-ray diffraction patterns and the results of the scanning electron microscopy (SEM) and energy dispersive X-ray spectroscopy (EDS) of the samples, we have identified all the phases that emerged in the samples. The experimental information gained on the phase equilibrium at 873 K is summarized in Table 2.

The micrographs of alloy 1# annealed at 873 K for 1800 hours are shown in Fig. 1. As a result of the SEM/EDS analysis, three phases have been determined, namely Fcc (Al), Al_3Y , Al_3Zr . This result is also confirmed by the XRD pattern in Fig. 3. As

shown in Fig. 1, the dark phase is an Al-based solid solution, light phase Al_3Zr dissolved with 2.14 at. % Y, and the gray phase is identified as $\text{Al}_3\text{Y}_\text{H}$. According to the binary phase diagram, $\text{Al}_3\text{Y}_\text{H}$ will transfer to $\text{Al}_3\text{Y}_\text{L}$ at 912 K, this observation in our results appears to be different from those reported in the literature. It was also reported by Dagerhamn [23] this phase transaction was difficult to take place. In the meantime, the first principle calculations are also applied to determine the energy difference between these two phases. The calculated formation enthalpies from first-principles calculations for $\text{Al}_3\text{Y}_\text{H}$ and $\text{Al}_3\text{Y}_\text{L}$ are -43 kJ/mol and -45 kJ/mol. The energy difference is quite small which leads to a small driving force for the $\text{Al}_3\text{Y}_\text{H}$ to $\text{Al}_3\text{Y}_\text{L}$ transition. We believe that $\text{Al}_3\text{Y}_\text{H}$ will transform to $\text{Al}_3\text{Y}_\text{L}$ only with increasing annealing times.



Figure 1. Backscattered electron images of alloy 1# $\text{Al}_{78.9}\text{Y}_{12.4}\text{Zr}_{8.8}$ at 873 K

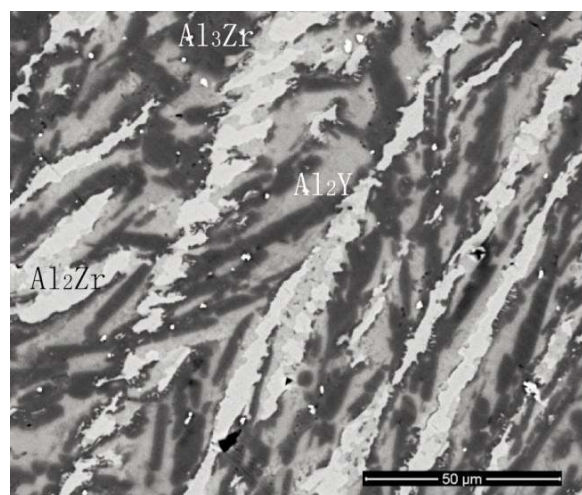


Figure 2. Backscattered electron images of alloy 2# $\text{Al}_{69.7}\text{Y}_{11.29}\text{Zr}_{19.01}$ at 873 K



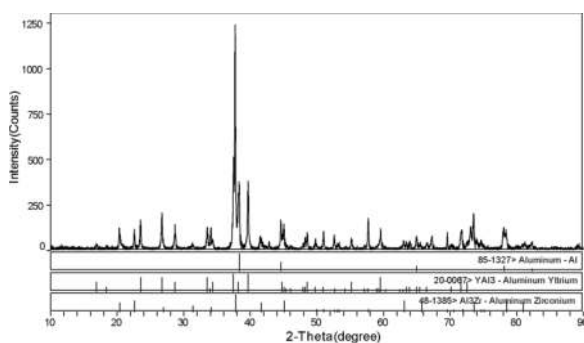


Figure 3. XRD patterns of alloy 1# $Al_{78.9}Y_{12.4}Zr_{8.8}$

The micrographs of alloys 2# annealed at 873 K for 1800 h are shown in Fig. 2. As a result of the SEM/EDS analysis, three phases have been found, namely Al_2Y , Al_2Zr , Al_3Zr . As shown in Fig. 2, the dark phase is Al_3Zr , light phase Al_2Zr , and the gray phase is identified as Al_2Y . In order to confirm the phases in this alloy, XRD measurements were conducted. The XRD pattern is listed in Fig. 4, which shows good agreement with the results from SEM/EDS.

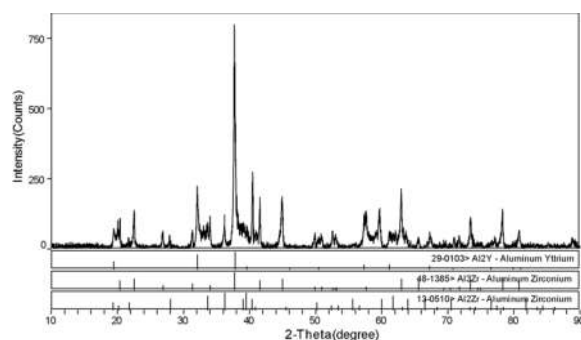


Figure 4. XRD patterns of alloy 2# $Al_{69.7}Y_{11.29}Zr_{19.01}$

With similar methods, phase analysis are also obtained, the results are listed in Table 2, which shows six three-phase regions in the Al-rich region of Al-Y-Zr system. No ternary compound could be found in this region, which is in agreement with the work of She et al. [16].

3.2 Solid solubility

Different from an earlier study [16], the solubility of the third element in the binary compounds cannot be ignored in our experiments. The solubility is found to be zero in the work of She et al. [16]. However, in our results, the maximum solubility of Zr in Al_3Y , Al_2Y and AlY phases are reported as 1.34, 9.25 and 5.48 at. % while the maximum solubility of Y in Al_3Zr , Al_2Zr , Al_3Zr_2 , $AlZr$ and Al_3Zr_4 phases are 2.56,

11.4, 6.365, 4.77 and 4.34 at. %. These experimental data are listed in Table 2. It is readily discernible that in most binary compounds, the measured Al composition does not change noticeably along the ternary extension of the binary phase excepted in the Al_2Y and Al_3Zr_2 phases.

Table 2. Measured equilibrium alloy compositions and phases at 873K for 1800 hours

No	EDX composition (at.%)			Phase	Compositions			Remark
	Al	Y	Zr		Al	Y	Zr	
1	78.8	12.38	8.82	Al_3Y	73.67	25.97	0.36	Tie-triangle
				Al_3Zr	73.605	2.14	24.26	
				Al	99.62	0.32	0.06	
2	69.7	11.29	19.01	Al_3Zr	72.75	2.25	25.01	Tie-triangle
				Al_2Y	64.76	25.98	9.25	
				Al_2Zr	64.27	3.65	32.08	
3	72.51	20.98	6.51	Al_2Y	68.15	23.47	8.39	Tie-triangle
				Al_3Y	73.19	25.465	1.34	
				Al_3Zr	73.21	2.56	24.23	
4	64.44	11.81	23.75	Al_2Zr	64.89	11.4	23.71	Tie-triangle
				Al_3Zr_2	59.125	6.365	34.51	
				Al_2Y	63.645	27.275	9.08	
5	52.31	18.97	28.72	Al_3Zr_2	57.92	3.07	39.02	Tie-triangle
				$AlZr$	48.46	4.14	47.43	
				AlY	47.77	46.75	5.48	
5	46.92	11.48	39.6	$AlZr$	48.66	4.34	47	Tie-triangle
				Al_3Zr_4	42.89	4.77	52.33	
				AlY	47.83	46.97	5.2	

3.3 Isothermal section

According to the experimental data in Table 2 and the phase analysis above, the partial isothermal section of the phase diagram of the Al-Y-Zr system at 873K has been constructed and is shown in Fig. 5. As shown in Fig. 5, the solid lines are acquired according to the present measurement and the dash line is extrapolated from the experimental results. Within the investigated composition ranges, 6 three-phase regions are determined at 873 K in this work, these are, $Al + Al_3Y + Al_3Zr$, $Al_3Zr + Al_2Y + Al_2Zr$, $Al_2Y + Al_3Y + Al_3Zr$, $Al_2Zr + Al_2Y + Al_3Zr_2$, $Al_3Zr_2 + AlZr + AlY$, $Al_3Zr_4 + AlZr + AlY$. No ternary compound was found in the present work which is in agreement with that of She et al. [16].

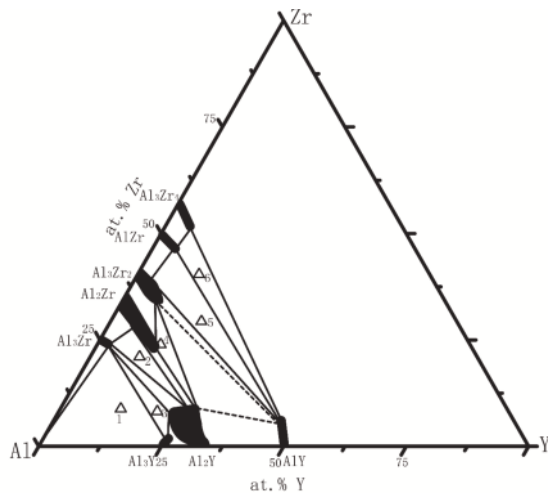


Figure 5. Isothermal section of Al-Y-Zr system at 873 K

4. Conclusion

The partial phase equilibria of the Al-Y-Zr system at 873 K has been systematically investigated by using XRD analysis, metallography and SEM/EDS composition measurement. Six three-phase regions are determined at 873 K in this work, which are Al + Al₃Y + Al₃Zr, Al₃Zr + Al₂Y + Al₂Zr, Al₂Y + Al₃Y + Al₃Zr, Al₂Zr + Al₂Y + Al₃Zr₂, Al₃Zr₂ + AlZr + AlY, Al₃Zr₄ + AlZr + AlY. Based on this work, the partial isothermal section of the phase diagram of Al-Y-Zr system at 873K has been constructed.

Acknowledgement

The authors would like to express gratitude to the financial support of the National Natural Science Foundation of China (Grant Num. 51371200, 51501229) and the Scientific Research Foundation for the Returned Overseas Chinese Scholars, State Education Ministry. Dr. Ligang Zhang would like thanks to Mr. Carl Meggs (University of Birmingham, Birmingham, B15 2TT, UK) for the useful discussions and language improvement.

References

- [1] N.Q. Vo, D.C. Dunand, D.N. Seidman, *Acta Materialia*, 63(2014) 73-85.
- [2] W. Jiang, Z. Fan, Y. Dai, C. Li, *Mater. Sci. Eng.: A*, 597(2014) 237-244.
- [3] X. Hu, F. Jiang, F. Ai, H. Yan, *J. Alloys Compd.*, 538(2012) 21-27.
- [4] X.H. Bao, L.B. Liu, Y.R. Jiang, Y. Jiang, C. Mao, X. Li, L.G. Zhang, *Journal of Phase Equilibria and Diffusion*, 37(2016), 345-349.
- [5] Y. Xu, J. Li, H. Zhang, Y. Lai, *Journal of Mining and Metallurgy B: Metallurgy*, 51(2015) 7-15.
- [6] L.G. Zhang, C. Schmetterer, P.J. Masset, *Computational Materials Science*, 66(2013) 20-27.
- [7] Z. Yin, Q. Pan, Y. Zhang, F. Jiang, *Mater. Sci. Eng.*, 280A (2000) 151-155.
- [8] L. Zhang L, P. Masset, F. Cao, F. Meng, L. Liu, Z. Jin, *J. Alloys Compd.*, 509(2011) 3822-3831.
- [9] L.G. Zhang, P.J. Masset, X.M. Tao, G.X. Huang, H.T. Luo, L.B. Liu, Z.P. Jin, *Calphad*, 35(2011) 574-579.
- [10] S. Lathabai, P.G. Lloyd, *Acta Materialia*, 50(2002) 4275-4292.
- [11] J.P. Huang, B. Yang, H.M. Chen, H. Wang, *J. Phase Equilib.*, 36(2015) 357-365.
- [12] Y. Kawazoe, J. Yu, A. Tsai, T. Masumoto, *Nonequilibrium Phase Diagrams of Ternary Amorphous Alloys*, Landolt Boernstein New Ser. Group III Condensed 199737.
- [13] H. Okamoto, *J. Phase Equilib.*, 23 (2002) 455-456.
- [14] K.A. Gschneidner Jr., F.W. Calderwood, *Bull. Alloy Phase Diagrams*, 10 (1) (1989).
- [15] A. Palenzona, S. Cirafici, *J. Phase Equilib.*, 12 (1991) 485-489.
- [16] J. She, Y. Zhan, Z. Hu, C. Li, J. Hu, *J. Alloys Compd.*, 497(2010) 118-120.
- [17] P.E. Blöchl, *Phys. Rev. B*, 50 (1994) 17953-17979
- [18] G. Kresse, D. Joubert, *Phys. Rev. B*, 59 (1999) 1758-1775
- [19] J.P. Perdew, K. Bucke, M. Ernzerhof, *Phys Rev Lett.*, 77(1996) 3865-3870
- [20] J. P. Perdew, K. Burke, M. Ernzerhof, *Phys. Rev. Lett.*, 78(1997) 1396.
- [21] G. Kresse, J. Furthmüller, *Phys. Rev. B*, 54 (1996) 11169-11186
- [22] G. Kresse, J. Furthmüller, *Comput. Mater. Sci.*, 6 (1996) 15-50
- [23] T. Dagerhamn, *Ark. Kemi*, 27(1967), 363-380.